Blowing Snow Sublimation and Transport over Antarctica from 11 Years of CALIPSO Observations

Stephen P Palm[1], Vinay Kayetha[1], Yuekui Yang[2] and Rebecca Pauly[1]

[1]Science Systems Applications Inc., 10210 Greenbelt Road, Greenbelt, Maryland USA 20771.

[2]NASA Goddard Space Flight Center, Greenbelt, Maryland USA 20771.

Address for all correspondence:

Stephen Palm, Code 612, NASA Goddard Space Flight Center, Greenbelt, Maryland USA 20771.

Email: stephen.p.palm@nasa.gov

Phone: +1-301-614-6276

ABSTRACT

Blowing snow processes commonly occur over the earth's ice sheets when the 10 m wind speed exceeds a threshold value. These processes play a key role in the sublimation and re-distribution of snow thereby influencing the surface mass balance. Prior field studies and modeling results have shown the importance of blowing snow sublimation and transport on the surface mass budget and hydrological cycle of high latitude regions. For the first time, we present continent-wide estimates of blowing snow sublimation and transport over Antarctica for the period 2006 - 2016 based on direct observation of blowing snow events. We use an improved version of the blowing snow detection algorithm developed for previous work that uses atmospheric backscatter measurements obtained from the CALIOP (Cloud-Aerosol Lidar with Orthogonal Polarization) lidar aboard the CALIPSO (Cloud-Aerosol Lidar and Infrared Pathfinder Satellite Observation) satellite. The blowing snow events identified by CALIPSO and meteorological fields from MERRA-2 are used to compute the blowing snow sublimation and transport rates. Our results show that maximum sublimation occurs along and slightly inland of the coastline. This is contrary to the observed maximum blowing snow frequency which occurs over the interior. The associated temperature and moisture re-analysis fields likely contribute to the spatial distribution of the maximum sublimation values. However, the spatial pattern of the sublimation rate over Antarctica is consistent with modeling studies and precipitation

estimates. Overall, our results show that the 2006 – 2016 Antarctica average integrated blowing snow sublimation is about 393 ± 196 Gt yr^{-1} which is considerably larger than previous model-derived estimates. We find maximum blowing snow transport amount of 5 Megatons km^{-1} yr^{-1} over parts of East Antarctica and estimate that the average snow transport from continent to ocean is about 3.7 Gt yr^{-1}. These continent-wide estimates are the first of their kind and can be used to help model and constrain the surface-mass budget over Antarctica.

Keywords: Blowing snow, sublimation, transport, CALIPSO, Antarctica, surface mass balance

1 Introduction

The surface mass balance of the earth's great ice sheets that cover Antarctica and Greenland is one of today's most important topics in climate science. The processes that contribute to the mass balance of a snow or ice-covered surface are precipitation (P), surface evaporation and sublimation (E), surface melt and runoff (M), blowing snow sublimation (Q_s) and snow transport (Q_t). Sublimation of snow can occur at the surface but is greatly enhanced within the atmospheric column of the blowing snow layer. The contributions of these processes to the mass balance vary greatly spatially, and can be highly localized and very difficult to quantify.

$$S = \int_{year} (P - E - M - Q_t - Q_s)dt \quad (1)$$

It is well known that the Arctic is experiencing rapid warming and loss of sea ice cover and thickness. In the past few decades, the Arctic has seen an increase in average surface air temperature by 2 °C (Przybylak, 2007). Modeling studies suggests an increase in annual mean temperatures over the Arctic by 8.5 ± 4.1 °C over the current century that could lead to a decrease in sea ice cover by 49 ± 18 % (Bintanja and Krikken, 2016). While the Antarctic has experienced an increase in average surface temperature, most of the warming is observed over West Antarctica at a rate of 0.17 °C per decade from 1957 to 2006 (Steig et al., 2009; Bromwich et al., 2013). Such surface warming undoubtedly has implications for ice sheet mass balance and sea level rise mainly through the melting term of the mass balance equation. However, the other processes affecting the mass balance of ice sheets may also be experiencing changes that

are difficult to identify and quantify. For instance, models have shown that in a warming climate, precipitation should increase over Antarctica and most of it will fall as snow (Church et al., 2013). If snowfall is increasing, perhaps the frequency of blowing snow and subsequently the magnitude of transport and sublimation will increase as well. Thus, understanding how these processes affect the overall mass balance of the ice sheets and how they may be responding to a changing climate is of growing concern.

In addition to ice sheet mass balance, sublimation of blowing snow is also important for the atmospheric moisture budget in high latitudes. For instance, in the Canadian Prairies and parts of Alaska sublimation of blowing snow was shown to be equal to 30 % of annual snowfall (Pomeroy et al., 1997). About 50 % of the wind-transported snow sublimates in the high plains of southeastern Wyoming (Tabler et al., 1990). Adequate model representation of sublimation processes are important to obtain reliable prediction of spring runoff and determine the spatial distribution/variability of energy and water fluxes and their subsequent influence on atmospheric circulation in high latitude regions (Bowling et al., 2004).

Over Antarctica, blowing snow occurs more frequently than anywhere else on earth. Models driven by long-term surface observations over the Neumayer station (East Antarctica), estimate that blowing snow sublimation removes up to 19 % of the solid precipitation (Van den Broeke et al., 2010). Over certain parts of the Antarctica, where persistent katabatic winds prevail, blowing snow sublimation is found to remove up to 85 % of the solid precipitation (Frezzotti et al., 2002). Over coastal areas up to 35% of the precipitation may be removed by wind through transport and sublimation (Bromwich 1988). Das et al., (2013) concluded that ~ 2.7–6.6 % of the surface area of Antarctica has persistent negative net accumulation due to wind scour (erosion and sublimation of snow). These studies show the potential role of the blowing snow sublimation process in the surface mass balance of the earth's ice sheets.

For the current work, we focus on blowing snow processes over the Antarctic region. Due to the uninhabited expanse of Antarctica and the lack of observations, prior, continent-wide studies of blowing snow sublimation over Antarctica had to rely on parameterized methods that use model re-analysis of wind speed and low level moisture. The presence of blowing snow is inferred from surface temperature, wind speed and snow age (if known). In a series of papers

on the modeling of blowing snow, Dery and Yau (1998, 1999, 2001) develop and test a parameterization of blowing snow sublimation. Dery and Yau (2002) utilize the model with the ECMWF re-analysis covering 1979 to 1993 and show that most blowing snow sublimation occurs along the coasts and over sea ice with maximums in some coastal areas of 150 mm snow water equivalent (swe) yr^{-1}. Lenearts et al., (2012a) utilized a high resolution regional climate model (RACMO2) to simulate the surface mass balance of the Antarctic ice sheet. They found drifting and blowing snow sublimation to be the most significant ablation term reaching values as high as 200 mm yr^{-1} swe along the coast. Average monthly rates of blowing snow sublimation calculated for Halley Station, Antarctica for the years 1995 and 1996, varied between 0.04 (winter) to 0.44 (summer) mm day^{-1} (14.6 and 160 mm yr^{-1} respectively) (King et al. 2001). There has been some recent work done on blowing snow sublimation and transport from field measurements (see for instance Barral et al.,2014 and Trouvilliez et. al., 2014) , but the data are sparse and measurements are only available within the surface layer (< 10 m).

While transport of blowing snow is considered to be less important than sublimation in terms of mass balance of the Antarctic ice sheet, erosion and transport of snow by wind can be considerable in certain regions. Das et al., (2013) have shown that blue ice areas are frequently seen in Antarctica. These regions exhibit a negative mass balance as all precipitation that falls is either blown off or sublimated away. Along the coastal regions it has been argued that considerable mass is transported off the coast via blowing snow in preferential areas dictated by topography (Scarchilli et al., 2010). In the Tera Nova Bay region of East Antarctica, manned surface observations show that drifting and blowing snow occurred 80 % of the time in fall and winter and cumulative snow transport was 4 orders about of magnitude higher than snow precipitation. Much of this airborne snow is transported off the continent producing areas of blue ice. Such observations raise questions as to how often and to what magnitude continent to ocean transport occurs. This is important, particularly for Antarctica where the coastline stretches over 17,000 km in length (https://en.wikipedia.org/wiki/Antarctica) and where prevailing strong winds occur through most of the year. Due to the sparsity of observations, the only way to estimate the mass of snow being blown off the coast of Antarctica is by using

model parameterizations. Now, for the first time, satellite observations of blowing snow can help better ascertain the magnitude of this elusive quantity.

Considering that the accuracy of model data is questionable over Antarctica, and the complicated factors that govern the onset of blowing snow, it is difficult to assess the accuracy of the parameterization of blowing snow sublimation and transport. Recently, methods have been developed to detect the occurrence of blowing snow from direct satellite observations. Palm et al., (2011) show that blowing snow is widespread over much of Antarctica and, in all but the summer months, occurs over 50 % of the time over large areas of East Antarctica. In this paper, we present a technique that uses direct measurements of blowing snow from the CALIPSO satellite lidar combined with The Modern-Era Retrospective analysis for Research and Applications, Version 2 (MERRA-2) re-analysis fields of moisture, temperature and wind to quantify the magnitude of sublimation and mass transport occurring over most of Antarctica (north of 82 south). Section 2 discusses the method used to compute blowing snow sublimation from CALIPSO and MERRA-2 data. In Sect. 3 we show results and compare with previous estimates of sublimation. In Sect. 4 we examine sources of error, their approximate magnitudes and perform a study on the sensitivity of the calculated sublimation to error in the estimated relative humidity of the layer. Summary and discussion follow in Sect. 5.

2 Method

The method developed for detection of blowing snow using satellite lidar data (both ICESat and CALIPSO) was presented in Palm et al., (2011). That work showed examples of blowing snow layers as seen by the calibrated, attenuated backscatter data measured by the CALIOP instrument on the CALIPSO satellite. CALIOP (Cloud-Aerosol Lidar with Orthogonal Polarization) is a two wavelength (532 and 1064 nm) backscatter lidar with depolarization at 532 nm and has been operating continuously since June of 2006 (Winker et. al., 2009). In the lower 5 km of the atmosphere, the vertical resolution of the CALIOP backscatter profile is 30 m. The CALIOP backscatter profiles are produced at 20 Hz, which is about a horizontal resolution of 330 m along track. The relatively strong backscattering produced by the earth's surface is used to identify the ground bin in each profile. After the ground signal is detected, each 20 Hz profile is

examined for an elevated backscatter signal (above a pre-defined threshold) in the first bin above the ground. If found and the surface wind speed is greater than 4 m s^{-1}, successive bins above that are searched for a 80 % decrease in signal value, which is then the top of the layer. Limited by the vertical resolution of the signal, our approach has the ability to identify blowing snow layers that are roughly 20-30 m or more in thickness. Thus, drifting snow which is confined to 10 m or less and occurs frequently over Antarctica would not be reliably detected. The signal from these layers is likely inseparable from the strong ground return. More information on the blowing snow detection algorithm can be found in Palm et al., (2011).

For the work done in this paper we have created a new version of the blowing snow detection algorithm which strives to reduce the occurrence of false positive blowing snow detections. This is done by looking at both the layer average 532 nm depolarization ratio and color ratio (1064/532) and limiting the top height of the layer to 500 m. If a layer is detected, but the top of the layer is above 500 m, it is not included as blowing snow. This height limit helped screen out diamond dust which often stretches for a few kilometers vertically and frequently reaches the ground. It was found that for most blowing snow layers, the depolarization and color ratio averaged about 0.4 and 1.3, respectively (see Fig. 1). If the layer average color or depolarization ratios were out of pre-defined threshold limits, the layer was rejected. The layer average color ratio had to be greater than 1.0 and the depolarization ratio greater than 0.25. The large color ratio is consistent with model simulations for spherical ice particles (Bi et al., 2009). Further, logic was included to reduce misidentification of low cloud as blowing snow by limiting both the magnitude and height of the maximum backscatter signal in the layer. If the maximum signal were greater than 2.0×10^{-1} km^{-1} sr^{-1}, the layer was assumed cloud and not blowing snow. In addition, if the maximum backscatter, regardless of its value, occurs above 300 m, the layer is rejected. These changes to the blowing snow detection algorithm slightly decreased (few percent) the overall frequency of blowing snow detections, but we believe we have reduced the occurrence of false positives and the resulting retrievals are now more accurate.

Typically, the blowing snow layers are 100–200 m thick, but can range from the minimum detectable height (20 - 30 m) to over 400 m in depth (Mahesh et al., 2003). Often they are seen

to be associated with blowing snow storms that cover vast areas of Antarctica and can persist for days. Blowing snow can occur as frequently as 50 % of the time over large regions of East Antarctica in all months but December–February and as frequently as 75 % April through October (Palm et al., 2011). An example of a typical blowing snow layer as seen from the CALIOP backscatter data is shown in Fig. 1.

2.1 MERRA-2 Reanalysis Data

In order to compute blowing snow sublimation, the temperature and relative humidity of the layer must be known. Here we use the MERRA-2 reanalysis (Gelaro, 2017). MERRA-2 is produced with version 5.12.4 of the GEOS atmospheric data assimilation system and contains 72 vertical levels from the surface to 0.01 hPa on an approximately 0.5° x 0.625° global grid. The re-analyses are available every 3 hours. To obtain the temperature and relative humidity at a given location, height and time, we use the data from the MERRA-2 grid box which is closest in space and time to the observation. Then we linearly interpolate the temperature, moisture and wind to the height of the CALIPSO observation.

MERRA-2 does not include the effects of blowing snow sublimation on atmospheric moisture and thus may have a dry (and possibly warm) bias. MERRA-2 temperature and moisture has not been evaluated over Antarctica but in this section we present a comparison of MERRA-2 temperature and moisture at 2 m height with a manned surface station (princess Elisabeth Station) and six AWS sites. In supplemental Figs. S1 – S6 are data from the AWS sites comparing MERRA-2 and AWS 2 m temperature and relative humidity with respect to ice (RHice). In all but one case MERRA-2 is, on average, slightly colder than the observations (about 3 °C). For all six comparisons, the average MERRA-2 moisture is greater than the AWS observation (roughly 7% higher).

Supplemental Figs. S7 and S8 show MERRA-2 data compared to the surface station at Princess Elisabeth (PE) for data taken over 2009-2015. Princess Elisabeth Station is located in East Antarctica at 71.95S, 23.35E at an elevation of 1322m. The PE surface observations are made year round at 3 hourly intervals. MERRA-2 data is then extracted at the time closest to the PE observation. Both the MERRA-2 and the PE data are then averaged over the month. The result

shown in Figs. S7 and S8 indicate that MERRA-2 is consistently colder and moister than the observations (about 6.1 °C and-8.4%, respectively). Note also from Fig. S8 that MERRA-2 is much colder than the observations in winter and somewhat closer to observations in the summer. The bias shown in Figs. S1 - S7 is calculated as the average of the MERRA-2 data minus the average of the station data. Also shown in Fig. S9 are the annual mean relative humidity at 2 meters above the surface over Antarctica in 2015 estimated by MERRA-2, ERA-Interim, and AMPS-Polar WRF showing that MERRA-2 is considerably moister than ERA-Interim or AMPS. Note that the model humidity fields shown in Fig. S9 are with respect to water.

From these comparisons it is likely that MERRA-2 does not exhibit a dry or warm bias and is rather slightly cold and moist compared to surface observations and other models.

2.2 Sublimation

Sublimation of snow occurs at the surface but is greatly enhanced when the snow becomes airborne by the action of wind and turbulence. Once snow particles become airborne, their total surface area is exposed to the air. If the relative humidity of the ambient air is less than 100 %, then sublimation will occur. The amount of sublimation is dictated by the number of snow particles in suspension and the relative humidity and temperature of the air. Thus, to estimate sublimation of blowing snow, we must be able to derive an estimate of the number density of blowing snow particles and have knowledge of atmospheric temperature and moisture within the blowing snow layer. The only source of the latter, continent wide at least, is from global or regional models or re-analysis fields. The number density of blowing snow particles can be estimated directly from the CALIOP calibrated, attenuated backscatter data if we can estimate the extinction within the blowing snow layer and have a rough idea of the blowing snow particle radius. The extinction can be estimated from the backscatter through an assumed extinction to backscatter ratio (lidar ratio) for the layer. The lidar ratio, though unknown, would theoretically be similar to that of cirrus clouds, which has been extensively studied. Work done by Josset et al., (2012) and Chen et al., (2002) shows that the extinction to backscatter ratio for cirrus clouds typically ranges between 25 and 30 with an average value of 29. However, the ice particles that make up blowing snow are more rounded than the ice

227 particles that comprise cirrus clouds and are on average somewhat smaller (Walden et al.,
228 2003). For this paper, we use a value of 25 for the extinction to backscatter ratio.

229 Measurements of blowing snow particle size have been made by a number of investigators
230 [Schmidt, 1982; Mann et al., 2000; Nishimura and Nemoto, 2005; Walden et al. 2003; Lawson et
231 al., 2006; Gordon and Taylor, 2009], but they were generally made within the first few meters
232 of the surface and may not be applicable to blowing snow layers as deep as those studied here.
233 Most observations have shown a height dependence of particle size ranging from 100 to 200
234 μm in the lower tens of centimeters above the surface to 50–60 μm near 10 m height
235 (Nishimura and Nemoto, 2005). A notable exception is the result of Harder et al., (1996) at the
236 South Pole, who measured the size of blowing snow particles during a blizzard by collecting
237 them on a microscope slide. They report nearly spherical particles with an average effective
238 radius of 15 μm, but the height at which the measurements were made is not reported. From
239 surface observations made at the South Pole, Walden et al., (2003) and Lawson et al., (2006)
240 report an average effective radius for blowing snow particles of 19 and 17 μm, respectively.

241 While no field-measured values for particle radii above roughly 10 m height are available,
242 modeling work indicates that they approach an asymptotic value of about 10-20 μm at heights
243 of 200 m or more (Dery and Yau, 1998). It is also reasonable to assume that snow particles that
244 are high up in the layer are smaller since they have spent more time aloft and have had a
245 greater time to sublimate. Based on the available data, we have defined particle radius (*r(z)*,
246 μm) as a linear function of height:

247 $$r(z) = 40 - \frac{z}{20} \quad (1)$$

248 Thus, for the lowest level of CALIPSO retrieved backscatter (taken to be 15 m – the center of
249 the first bin above the surface), r(15) = 39.25 μm and at the highest level (500 m), r(500) = 15
250 μm.

251 The blowing snow particle number density *N(z)* (particles per cubic meter) can be estimated
252 from the extinction. Note that the extinction is the numerator in equation 2:

$$N(z) = \frac{(\beta(z) - \beta_m(z))\, S}{2\pi\, r^2(z)} \quad (2)$$

Where $\beta(z)$ is the CALIPSO measured attenuated calibrated backscatter at height z (30 m resolution), $\beta_m(z)$ is the molecular backscatter at height z and S is the extinction to backscatter ratio (25). Here $\beta(z)$ represents the atmospheric backscatter profile through the blowing snow layer. Both $\beta_m(z)$ and $\beta(z)$ have units of m^{-1} sr^{-1}. We found that the values of N(z) obtained from Eq. (2) for the typical blowing snow layer range from about 5.0×10^4 to 1.0×10^6 particles per cubic meter. This is consistent with the blowing snow model results of Dery and Yau (2002) and the field observations of Mann et al., (2000). A plot of the average particle density for the blowing snow layer in Fig. 1 is shown in Fig. 2. Note that the decrease in particle number density below about 75 m is most likely due to attenuation of the lidar signal as it propagates through the layer. We did not attempt to correct for this and the overall effect is an under estimation of the particle density in this region (which would lead to lower calculated blowing snow sublimation).

Once an estimate of blowing snow particle number density and radii are obtained, the sublimation rate of the particles can be computed based on the theoretical knowledge of the process. Following Dery and Yau, (2002), the blowing snow mixing ratio q_b (kg ice / kg air) is given by:

$$q_b(z) = \frac{4\pi\, \rho_{ice}\, r^3(z)\, N(z)}{3\, \rho_{air}} \quad (3)$$

Or substituting for $N(z)$ (Eq. 2):

$$q_b(z) = \frac{2\, \rho_{ice}\, r(z)\, [\beta(z) - \beta_m(z)]\, S}{3\, \rho_{air}} \quad (4)$$

Where ρ_{ice} is the density of ice (917 kg m^{-3}), and ρ_{air} the density of air. Again following Dery and Yau (2002) and others, the sublimation S_b at height z is computed from:

$$S_b(z) = \frac{q_b(z)\, N_u\, [q_v(z)/q_{is}(z) - 1]}{2\, \rho_{ice}\, r^2(z)\, [F_k(z) + F_d(z)]} \quad (5)$$

Or, letting $\alpha(z)$ be the extinction and substituting for $q_b(z)$:

$$S_b(z) = \frac{\alpha(z)\, N_u\, [q_v(z)/q_{is}(z) - 1]}{3\, \rho_{ice}\, r(z)\, [F_k(z) + F_d(z)]} \quad (6)$$

Where Nu is the Nusslet number defined as: $Nu = 1.79 + 0.606\, Re^{0.5}$

with the Reynolds number being: $Re = 2r(z)\ v_b/v$

where v_b is the snow particle fall speed (assumed here to be 0.1 ms^{-1}) and v the kinematic viscosity of air (1.512x10^{-5} m^2s^{-1}). q_v is the water vapor mixing ratio of the air (obtained from model data), q_{is} is the saturation mixing ratio with respect to ice, and F_k and F_d are the heat conduction and diffusion terms (m s kg^{-1}):

$$F_k = \left(\frac{L_s}{R_v T} - 1\right)\ \frac{L_s}{KT} \quad (7)$$

$$F_d = \frac{R_v T}{D\ e_i(T)} \quad (8)$$

Where L_s is the latent heat of sublimation (2.839x10^6 J/Kg), R_v is the individual gas constant for water vapor (461.5 J kg^{-1} K^{-1}), T is temperature (K), *K* is the thermal conductivity of air, and *D* the coefficient of diffusion of water vapor in air (both *D* and *K* are functions of temperature (see Rogers and Yau, 1989). S_b has units of kg kg^{-1} s^{-1}. This can be interpreted as the mass of snow sublimated per mass of air per second.

Then the column integrated blowing snow sublimation is:

$$Q_s = \rho_{air}\ \int_{z=0}^{Z_{top}} S_b(z)\, dz \quad (9)$$

Where Z_{top} is the top of the blowing snow layer and *dz* is 30 meters. Q_s has units of kg m^{-2} s^{-1}). Conversion to mm snow water equivalent (swe) per day is performed by multiplying by a conversion factor:

$$\rho' = 10^3\ \ N_s/\rho_{ice}(1) \quad (10)$$

Where N_s is the number of seconds in a day (86,400). The total sublimation amount in mm swe per day is then:

$$Q' = \rho' \, Q_s \tag{11}$$

This computation is performed for every blowing snow detection along the CALIPSO track over Antarctica. A 1 x 1 degree grid is then established over the Antarctic continent and each sublimation calculation (*Q'*) is added to its corresponding grid box over the length of time being considered (i.e. a year or month). This value is then normalized by the total number of CALIPSO observations that occurred for that grid box over the time span. The total number of observations includes all CALIPSO shots within the grid box for which a ground return was detected, regardless of whether blowing snow was detected for that shot or not. Thus, the normalization factor is the total number of shots with ground return detected for that box and is always greater than the number of blowing snow detections (which equals the number of sublimation retrievals). In order for the blowing snow detection algorithm to function, it must first detect the position of the ground return in the backscatter profile. If it cannot do so, it is not considered an observation. Over the interior of Antarctica, failure to detect the surface does not occur often as cloudiness is less than 10 % and most clouds are optically thin. Near the coasts, optically thick clouds become more prevalent. This approach will result in higher sublimation values for those grid boxes that contain a lot of blowing snow detections and vice versa (as opposed to just taking the average of the sublimation values for a grid box).

2.3 Transport

The transport of blowing snow is computed using the CALIPSO retrievals of blowing snow mixing ratio and the MERRA-2 winds. A transport value is computed at each 30 m bin level and integrated through the depth of the blowing snow layer:

$$Q_t = \rho_{air} \int_{z=0}^{Z_{top}} q_b(z) \; u(z) \; dz \tag{12}$$

Where $q_b(z)$ is the blowing snow mixing ratio from Eq. (3) and $u(z)$ is the MERRA-2 wind speed at height z and Q_t has units of kg m^{-1} s^{-1}. The wind speed is linearly interpolated from the nearest two model levels. As with the sublimation, these values are gridded and normalized by the total number of observations. The transport values are computed for each month of the year by summing daily values and then multiplying by the number of seconds in the month (resulting units of kg m^{-1}). The monthly values are then summed to obtain a yearly amount. A further conversion is performed to produce units of Gt m^{-1} yr^{-1} by dividing by 10^{12} (1000 kg per metric ton and 10^9 tons per Gt).

3 Results

3.1 Sublimation

Fig. 3 shows the average blowing snow frequency and corresponding total annual blowing snow sublimation over Antarctica for the period 2007–2015. The highest values of sublimation are along and slightly inland of the coast. Notice that this is not necessarily where the highest blowing snow frequencies are located. Sublimation is highly dependent on the air temperature and relative humidity. For a given value of the blowing snow mixing ratio (q_b), the warmer and drier the air, the greater the sublimation. In Antarctica, it is considerably warmer along the coast but one would not necessarily conclude that it is drier there. However, other authors have noted that the katabatic winds, flowing essentially downslope, will warm and dry the air as they descend (Gallee, 1998, and others). We have examined the MERRA-2 relative humidity (with respect to ice) and indeed, according to the model, it is usually drier along the coast. The model data often shows 90 to 100 % (or even higher) relative humidity for interior portions of Antarctica, while along the coast it is often 70 % or less. It should be noted, however, that this model prediction has never been validated through observations. The combination of warmer and drier air makes a big difference in the sublimation as shown in Fig. 4. For a given relative humidity the sublimation can increase by almost a factor of 100 as temperature increases from -50 to -10 °C. For temperatures greater than -20 °C, sublimation is very dependent on relative humidity, but this dependence lessens somewhat at colder temperatures. Continental interior

areas with very high blowing snow frequency that approach 75 % (like the Mega Dune region in East Antarctica) exhibit fairly low values of sublimation because it is very cold and the model relative humidity is high.

Fig. 5 shows the annual total sublimation for years 2007–2015. It is evident that the sublimation pattern or magnitude does not change much from year to year. The overall spatial pattern of sublimation is similar to the model prediction of Dery and Yau, (2002) with our results showing noticeably greater amounts in the Antarctic interior and generally larger values near the coast. As previously noted, most sublimation occurs near the coast due mainly to the warmer temperatures. The areas of sublimation maximums near the coast are consistently in the same location year to year, indicating that these areas may experience more blowing snow episodes and possibly more precipitation (availability of snow to become airborne). It is interesting to compare the sublimation pattern with current estimates of Antarctic precipitation. Precipitation is notoriously difficult to quantify over Antarctica due to the scarcity of observations and strong winds producing drifting and blowing snow which can be misidentified as precipitation. Precipitation is often measured by looking at ice cores or is estimated by models. But perhaps the most complete (non-model) measure of Antarctic precipitation come from the CloudSat mission. Palerme et al., (2014) used CloudSat data to construct a map of Antarctic precipitation over the entire continent (north of 82 S). They showed that along the East Antarctic coast and slightly inland, precipitation ranges from 500 to 700 mm swe yr^{-1} and decreases rapidly inland to less than 50 mm yr^{-1} in most areas south of 75 S. Their precipitation pattern is in general agreement with the spatial pattern of our sublimation results and the magnitude of our sublimation estimates is in general less than the precipitation amount, with a few exceptions. These occur mostly inland in regions of high blowing snow frequency such as the Megadune region and in the general area of the Lambert glacier. In these regions, our sublimation estimates exceed the CloudSat yearly precipitation estimates. When this occurs, it is likely that either the precipitation estimate is low or the sublimation estimate is too high. Otherwise it would indicate a net negative mass balance for the area unless transport of snow into the region accounted for the difference.

Table 1 shows the average sublimation over all grid cells in snow water equivalent and the integrated sublimation amount over the Antarctic continent (north of 82S) for the CALIPSO period in Gt yr^{-1}. Note that the 2006 data include only months June–December (CALIOP began operating in June, 2006) and the 2016 data are only up through October, and do not include the month of February (CALIOP was not operating). To obtain the integrated amount, we take the year average swe (column 1) multiplied by the surface area of Antarctica north of 82S and the density of ice. The average integrated value for the 9 year period 2007–2015 of 393 Gt yr^{-1} is significantly greater than (about twice) values in the literature obtained from model parameterizations (Lenaerts 2012b). Note also that this amount does not include the area poleward of 82S, the southern limit of CALIPSO observations. If included, and the average sublimation rate over this area were just 4 mm swe per year, this would increase the sublimation total by 10 Gt yr^{-1}. Palerme et al., (2014) has shown that the mean snowfall rate over Antarctica (north of 82 S) from August 2006 to April 2011 is 171 mm yr^{-1}. The average yearly snow water equivalent sublimation from Table I is the average sublimation over the continent (and grounded ice shelves) north of 82 S. For the same time period, our computed CALIPSO-based average blowing snow sublimation is about 50 mm yr^{-1}. This means that on average, over one third of the snow that falls over Antarctica is lost to sublimation through the blowing snow process. In comparison surface sublimation (sublimation of snow on the surface) is considered to be relatively small (about a tenth of airborne sublimation) except in summer (Lenearts 2012a, 2012b).

3.2 Transport

Transport of snow via the wind is generally important locally and does not constitute a large part of the ice sheet mass balance in Antarctica. There are areas where the wind scours away all snow that falls producing a net negative mass balance (i.e. blue ice areas), but in general, the snow is simply moved from place to place over most of the continent. At the coastline, however, this is not the case. There, persistent southerly winds can carry airborne snow off the continent. This can be seen very plainly in Fig. 6 which is a MODIS false color (RGB = 2.1, 2.1, .85 μm) image of a large area of blowing snow covering an area about the size of Texas (16,662

405 km^2) in East Antarctica. We have found this false color technique to be the best way to visualize
406 blowing snow from passive sensors. The one drawback is that sunlight is required. In Fig. 6,
407 blowing snow shows up as a dirty white, the ice/snow surface (in clear areas) is blue and clouds
408 are generally a brighter white. Also shown in Fig. 6 are two CALIPSO tracks (yellow lines) and
409 their associated retrieved blowing snow backscatter (upper and lower images of CALIOP
410 backscatter). Note that the yellow track lines are drawn only where blowing snow was detected
411 by CALIOP and that not all the CALIOP blowing snow detections are shown. The green dots
412 denote the coastline. Plainly seen along the coast near longitude 145–150E is blowing snow
413 being carried off the continent. In this case, topography might have played a role to funnel the
414 wind in those specific areas. Fig. 7 shows a zoomed in image of this area with the red lines
415 indicating the approximate position of the coastline. Also note that, as evidenced by the times
416 of the MODIS images, this transport began on or before October 13 at 23:00 UTC and continued
417 for at least 7 hours. This region is very close to the area of maximum sublimation seen in Fig. 3
418 and shown to be quite stable from year to year in Fig. 5. Undoubtedly, this continent to ocean
419 transport also occurs in other coastal areas of Antarctica and most often during the dark winter
420 (when MODIS could not see it).

421 In an attempt to better understand the magnitude of this phenomena, we have computed the
422 amount of snow mass being blown off the continent by computing the transport at 342 points
423 evenly spaced (about 60 km apart) along the Antarctic coast using only the v component of the
424 wind. If the v component is positive, then the wind is from south to north. The transport (Eq.
425 (12) using only the v wind component) is computed at each coastal location and then summed
426 over time at that location. The resulting transport is then summed over each coastal location to
427 arrive at a continent-wide value of transport from continent to ocean. Of course this assumes
428 that the coastline is oriented east-west everywhere. This is true of a large portion of Antarctica
429 but there are regional exceptions. Thus we view the results shown in Table II to be an upper
430 limit of the actual continent to ocean transport. Evident from Table II is that most of the
431 transport for East Antarctica occurs in a relatively narrow corridor, with on average over half
432 (51 %) of the transport occurring between 135E and 160E. This is obviously due to the very
433 strong and persistent southerly winds (see Fig. S10 and S11) and high blowing snow frequency

in this region and is consistent with the conclusions of Scarchilli et al., (2010). In West Antarctica, an even greater fraction (60 %) of the transport off the coast occurs between 80W and 120W.

In Fig. 8 we show the magnitude of blowing snow transport for the 2007–2015 timeframe in Mt km^{-1} yr^{-1} as computed from Eq. (12). The magnitude of snow transport, as expected, closely resembles the overall blowing snow frequency pattern as shown in Fig. 3. The maximum values (white areas in Fig. 8) exceed about 3 x 10^6 tons of snow per km per year. In the supplemental Figs. S10 and S11 we display the MERRA-2 average 10 m wind speed and direction for the years 2007–2015. By inspection of Figs. S10 and S11 it is seen that the overall transport in East Antarctica is generally from south to north and obviously dominated by the katabatic wind regime. It is immediately apparent that the average wind speed and direction does not change much from year to year, with the former helping to explain why the average continent-wide blowing snow frequency is also nearly constant from year to year (not shown).

4. Error Analysis

There are a number of factors that can affect the accuracy of the results presented in this work. These include:

1) Error in the calibrated backscatter and conversion to extinction
2) Errors in the assumed size of blowing snow particles
3) Not correcting for possible attenuation above and within the blowing snow layer
4) Misidentification of some layers as blowing snow when in fact they were not (false positives)
5) Failure to detect some layers (false negatives)
6) Errors in the MERRA-2 temperature and moisture data
7) Limited spatial sampling

The magnitude of some of these can be estimated, others are hard to quantify. For instance, 1), 2) and 6) are directly involved in the calculation of sublimation (Eq. 6). The error in extinction, particle radius, temperature and moisture can be estimated. The error associated with the

attenuation of the lidar signal above the blowing snow layer (3) is probably very small over the interior of Antarctica, but could be appreciable nearer the coastline. In the interior, clouds are a rare occurrence and when present are usually optically thin. Cloudiness increases dramatically near the coast both in terms of frequency and optical depth. Here the effect of overlying attenuating layers could be appreciable in that it would reduce the backscatter of the blowing snow layer and the derived extinction. This in turn would lead to a lower blowing snow mixing ratio and thus lower sublimation and transport. The effect of attenuation within the layer is unaccounted for here and will also reduce the amount of calculated blowing snow sublimation.

With regard to 5) above, the method presented here cannot reliably detect blowing snow layers less than 30 m thick. Therefore, sublimation associated with these layers is not accounted for. Other studies have shown that drifting snow sublimation within the salutation layer can be very significant (Huang et al., 2016). There is a further point to be made with respect to clouds that relates to 5) above. The method we use to detect blowing snow will not work in the presence of overlying, fully attenuating clouds. It is reasonable to suspect that cyclonic storms which impinge upon the Antarctic coast and travel some distance inland would be associated with optically thick clouds and contain both precipitating and blowing snow. Our method would not be able to detect blowing snow during these storms, but we would not count such cases as "observations", since the ground would not be detected. The point is, blowing snow probably occurs often in wintertime cyclones, but we are not able to detect it. This could lead to an under prediction of blowing snow occurrence, especially near the coast. Also, blowing snow layers less than 20 - 30 m thick would also likely be missed. It is not clear how often these layers occur, but they are known to exist and missing them will produce an underestimate of blowing snow sublimation and transport amounts. With regard to spatial sampling (7 above), unlike most passive sensors, CALIPSO obtains only point measurements along the spacecraft track at or near nadir. On a given day, sampling is poor. CALIPSO can potentially miss a large portion of blowing snow storms such as is evidenced from inspection of Fig. 6. We have seen many examples of such storms in both the MODIS and CALIPSO record. Quantifying the effect of poor sampling on sublimation estimates would be difficult but should be pursued in future work.

4.1 Sensitivity Analysis

A major limitation of this work is the uncertainty inherent in the meteorological data used for obtaining the temperature and moisture within the blowing snow layer. Re-analyses like MERRA-2 do not have the vertical or horizontal resolution to enable an accurate description of the temperature and moisture profile through the blowing snow layer. Also, as mentioned in section 2.1, MERRA-2, or more accurately the GEOS-5 model on which it is based, does not incorporate the effects of blowing snow sublimation on the moisture within the layer. Even so, we have already shown that MERRA-2 is moist compared to surface observations and to other models. Thus we do not feel that using the MERRA-2 moisture will cause a large overestimation of blowing snow sublimation. However, it is important to examine the effects of moisture on the calculated sublimation. To demonstrate this we have taken one CALIPSO track with blowing snow (shown in Fig. 9a) and plotted the MERRA-2 humidity (wrt ice) and the calculated blowing snow sublimation along the track. We then increased the moisture amount by 5 and 10% to see the effect on the calculated sublimation. The temperature was not changed. In Figs. 9b – 9d the MERRA-2 relative humidity is the dark solid line, MERRA-2 temperature is the dotted line and the calculated blowing snow sublimation is the thin black line. The temperature and moisture shown are the MERRA-2 averages through the blowing snow layer. Figure 9b shows the unperturbed MERRA-2 moisture and the resulting blowing snow sublimation (integrated through the layer). In Fig 9c and 9d we have increased the MERRA-2 relative humidity by 5 and 10%, respectively. The effect on the average blowing snow sublimation is marked. A 10% increase in relative humidity produces about a 30% reduction in the calculated blowing snow sublimation. This exercise demonstrates the non-linear effect of the moisture level on the calculated sublimation.

If we assume then that the error in moisture is 10%, we must accept that the resulting blowing snow sublimation could be 30% too high. But is that realistic, given the fact that the MERRA-2 data were shown to be moist compared to observation and other models (moister on average by 7%)? We do not think so. Rather we take the error in MERRA-2 moisture to be 5%. This produces an 18% over estimation of sublimation (Fig. 9b compared to Fig. 9c). This error must

be combined with other errors such as extinction, particle radius and temperature. Here we assume the extinction error to be 20 %, the particle radius error 10 % and the temperature error 5%. In Eq. (6) these terms are multiplicative. The total error in sublimation is then:

$$\pm 1 - (0.8 * 0.9 * 0.95) + 0.18 = \pm 0.50$$

This indicates that the sublimation values derived in this work should be considered to have an error bar of ±50 %. The error in computed transport involves error in wind speed and the blowing snow mixing ratio, the latter being dependent on extinction and particle size. If we assume wind speed has an error of 20 %, extinction 20 % and particle size 10 %, the total error in transport is:

$$\pm 1 - (0.8 * 0.8 * 0.9) = \pm 0.42$$

5. Summary and Discussion

This paper presents the first estimates of blowing snow sublimation and transport over Antarctica that are based on actual observations of blowing snow layers from the CALIOP space borne lidar onboard the CALIPSO satellite. We have used the CALIOP blowing snow retrievals combined with MERRA-2 model re-analyses of temperature and moisture to compute the temporal and spatial distribution of blowing snow sublimation and transport over Antarctica for the first time. The results show that the maximum sublimation, with annual values exceeding 250 (±125) mm swe, occurs within roughly 200 km of the coast even though the maximum frequency of blowing snow most often occurs considerably further inland. This is a result of the warmer and drier air near the coast which substantially increases the sublimation. In the interior, extremely cold temperatures and high model relative humidity lead to greatly reduced sublimation. However, the values obtained in parts of the interior (notably the Megadune region of East Antarctica - roughly 75 to 82S and 120 to 160E) are considerably higher than prior model estimates of Dery and Yau (2002) or Lenaerts et al., 2012a). This is most likely due to the very high frequency of occurrence of blowing snow as detected from CALIOP data in this region which is not necessarily captured in models (Lenaerts et al., 2012b).

542 The spatial pattern of the transport of blowing snow follows closely the pattern of blowing
543 snow frequency. The maximum transport values are about 5 Megatons per km per year and
544 occur in the Megadune region of East Antarctica with other locally high values at various
545 regions near the coast that generally correspond to the maximums in sublimation. We
546 attempted to quantify the amount of snow being blown off the Antarctic continent by
547 computing the transport along the coast using only the v component of the wind. While this
548 may produce an overestimate of the transport (since the Antarctic coast is not oriented east-
549 west everywhere), we find the amount of snow blown off the continent to be significant and
550 fairly constant from year to year. The average off-continent transport for the 9 year period
551 2007–2015 was 3.68 Gt yr^{-1} with about two thirds of that coming from East Antarctica and over
552 one third from a relatively small area between longitudes 135E and 160E.

553 Over the nearly 11 years of data, the inter-annual variability of continent wide sublimation
554 (Table 1) can be fairly large – 10 to 15 % - and likely the result of precipitation variability and or
555 changes in the MERRA-2 temperature and moisture data. There seems to be a weak trend to
556 the sublimation data with earlier years having greater sublimation than more recent years.
557 However, based on the short length of the time series and the likely magnitude of error in the
558 sublimation estimates, the trend cannot be considered statistically significant.

559 The overall spatial pattern of blowing snow sublimation is consistent with previous modelling
560 studies (Dery and Yau, 2002 and Lenearts et al., 2012a). However, we find the Antarctic
561 continent-wide integrated blowing snow sublimation to be larger than previous studies such as
562 Lenaerts et al., (2012a) (393 ±196 vs roughly 190 Gt yr^{-1}), even though the observations include
563 only the area north of 82° S. The maximum in sublimation is about 250 (±125) mm swe per year
564 near the coast between longitudes 140E and 150E and seems to occur regularly throughout the
565 11 year data record. There are a number of reasons for the higher sublimation values in this
566 study compared to prior estimates. 1) The depth of the layer: the average blowing snow layer
567 depth as determined from the CALIOP measurements is 120 m. Layers as high as 200 - 300 m
568 are not uncommon. It is likely that models such as those cited above do not always capture the
569 full depth of blowing snow layers, thus producing a smaller column-integrated sublimation

amount. 2) We only compute sublimation from blowing snow layers that are known to exist (meaning they have been detected from actual backscatter measurements). Models, on the other hand, must infer the presence of blowing snow from pertinent variables within the model. The existence of blowing snow is not easy to predict. It is a complicated function of the properties of the snowpack, surface temperature, relative humidity and wind speed. Snowpack properties include the dendricity, sphericity, grain size and cohesion, all of which can change with the age of the snow. In short, it is very difficult for models to predict exactly when and where blowing snow will occur, much less the depth that blowing snow layers will attain. 3) The lack of blowing snow physics within the MERRA-2 reanalysis. This produces perhaps the largest uncertainly in the derived results. It was shown that MERRA-2 is slightly colder and moister than some surface measurements and moister compared to other re-analyses. However, given the limited number of comparisons, a definitive conclusion on the accuracy of MERRA-2 data cannot be drawn. Since the model on which MERRA-2 re-analysis is based (GEOS-5) does not include blowing snow (and thus blowing snow feed backs on moisture and temperature), it is likely that our estimates of blowing snow sublimation are probably too high. However, the fact that we do not include blowing snow layers less than 30 m in depth and are not able to detect blowing snow beneath thick clouds layers means that we are missing potentially important contributions to sublimation. An addition, the retrieved blowing snow number density below about 80 m is probably too low for layers greater than 120 m in depth because of lidar signal attenuation. This will act to erroneously reduce the calculated sublimation. While we estimate an upper limit on the error of our blowing snow sublimation results as 50%, we believe that the error is considerably less than that.

Future work should involve coupling the CALIPSO blowing snow observations with a regional model that contains blowing snow physics. This could increase the accuracy of the calculated blowing snow sublimation by incorporating the moisture feedback processes within the layer that have been neglected here.

Data Availability

The CALIPSO calibrated attenuated backscatter data used in this study can be obtained from the NASA Langley Atmospheric Data Center at: https://earthdata.nasa.gov/about/daacs/daac-asdc

The MERRA-2 data are available from the Goddard Earth Sciences Data and Information Services Center (GESDISC) at: https://disc.gsfc.nasa.gov/datareleases/merra_2_data_release.

The blowing snow data (layer backscatter, height, etc.) are available through the corresponding author and will be made publicly available through the NASA Langley Atmospheric Data Center in the near future.

Acknowledgements

This research was performed under NASA contracts NNH14CK40C and NNH14CK39C. The authors would like to thank Dr. Thomas Wagner and Dr. David Considine for their support and encouragement. The CALIPSO data used in this study were the DOI: 10.5067/CALIOP/CALIPSO/LID_L1-ValStage1-V3-40_L1B-003.40 data product obtained from the NASA Langley Research Center Atmospheric Science Data Center. We also acknowledge the Global Modeling and Assimilation Office (GMAO) at Goddard Space Flight Center who supplied the MERRA-2 data. The authors appreciate the support of the University of Wisconsin-Madison Automatic Weather Station Program for the data set, data display, and information, NSF grant number ANT-1543305. We also acknowledge Alexandra Gossart of the Department of Earth and Environmental Sciences, KU Leuven, Leuven, Belgium for kindly supplying the surface observations taken at Princess Elisabeth Station, Antarctica.

References

Barral, H., C. Genthon, A. Trouvilliez, C. Brun, and C. Amory: Blowing snow in coastal Adélie Land, Antarctica: three atmospheric-moisture issues. The Cryosphere, 8, 1905–1919, 2014 www.the-cryosphere.net/8/1905/2014/ doi:10.5194/tc-8-1905-2014

Bi, L., Yang, P., Kattawar, G. W., Baum, B. A., Hu, Y. X., Winker, D. M., Brock, R. S., and J. Q. Lu, J. Q.: Simulation of the color ratio associated with the backscattering of radiation by ice particles

623 at the wavelengths of 0.532 and 1.064 μm, J. Geophys. Res., 114, D00H08,
624 doi:10.1029/2009JD011759, 2009.

625 Bintanja, R., and Krikken, F.: Magnitude and pattern of Arctic warming governed by the
626 seasonality of radiative forcing, Sci. Rep-Uk, 6, doi: 10.1038/srep38287, 2016.

627 Bowling, L. C., Pomeroy, J. W., and Lettenmaier, D. P.: Parameterization of blowing-snow
628 sublimation in a macroscale hydrology model, J Hydrometeor., 5, 745-762, doi: 10.1175/1525-
629 7541(2004)005<0745:Pobsia>2.0.Co;2, 2004.

630 Bromwich, D. H., Nicolas, J. P., Monaghan, A. J., Lazzara, M. A., Keller, L. M., Weidner, G. A., and
631 Wilson, A. B.: Central West Antarctica among the most rapidly warming regions on Earth, Nat.
632 Geosci., 6, 139-145, doi: 10.1038/Ngeo1671, 2013.

633 Bromwich, D. H.: Snowfall in high southern latitudes. Rev Geophys 26:149–168, 1988

634 Chen, W. N., Chiang, C. W., and Nee, J. B.: Lidar ratio and depolarization ratio for cirrus clouds,
635 Appl. Optics, 41, 6470-6476, doi: 10.1364/Ao.41.006470, 2002.

636 Church, J. A., Clark, P. U., Cazenave, A., Gregory, J. M., Jevrejeva, S., Levermann, A., Merrifield,
637 M. A., Milne, G. A., Nerem, R. S., Nunn, P. D., Payne, A. J., Pfeffer, W. T., Stammer, D., and
638 Unnikrishnan, A. S.: Sea level change, in: Climate change 2013: The Physical science basis.
639 Contribution of working group I to fifth assessment report of the Intergovernmental panel of
640 climate change, edited by: Stocker, T. F., Qin, D., Plattner, G. K., Tignor, M., Allen, S. K.,
641 Boschung, J., Nauels, A., Xia, Y., Bex, V., and Midgley, P. M., Cambridge University Press,
642 Cambridge, UK and New York, USA, 2013.

643 Das, I., Bell, R. E., Scambos, T. A., Wolovick, M., Creyts, T. T., Studinger, M., Frearson, N.,
644 Nicolas, J. P., Lenaerts, J. T. M., and van den Broeke, M. R.: Influence of persistent wind scour
645 on the surface mass balance of Antarctica, Nat. Geosci., 6, 367-371, doi: 10.1038/Ngeo1766,
646 2013.

647 Dery, S. J., and Yau, M. K.: Large-scale mass balance effects of blowing snow and surface
648 sublimation, J. Geophys. Res.-Atmos., 107, doi: 10.1029/2001jd001251, 2002.

649 Dery, S. J. and Yau, M. K.: Simulation of Blowing Snow in the Canadian Arctic Using a Double-
650 Moment Model, *Boundary-Layer Meteorology,* 99, 297–316, 2001.

651 Dery, S. J. and M.K. Yau, M. K.: A Bulk Blowing Snowmodel, *Boundary-Layer Meteorology,* 93,
652 237–251, 1999.

653 Dery, S. J., Taylor, P. A., Xiao, J.: The Thermodynamic Effects of Sublimating, Blowing Snow in
654 the Atmospheric Boundary Layer, Dept. of Atmospheric and Oceanic Sciences, McGill
655 University, 805 Sherbrooke St. W., Montréal, Québec, H3A 2K6 Canada, Boundary-Layer
656 Meteorology, 89, 251–283, 1998.

657 Frezzotti, M., Gandolfi, S., and Urbini, S.: Snow megadunes in Antarctica: Sedimentary structure
658 and genesis, J. Geophys. Res.-Atmos., 107, doi: 10.1029/2001jd000673, 2002.

659 Gallée, H.: A simulation of blowing snow over the Antarctic ice sheet, Ann Glaciol, 26, 203–205,
660 1998.

661 Gelaro, R., W. McCarty, M. Suarez, R. Todling, A. Molod, L. Takacs, C. Randles, A. Darmenov, M.
662 Bosilovich, R. Reichle, K. Wargan, L. Coy, R. Cullather, C. Draper, S. Akella, V. Buchard, A. Conaty,
663 A. da Silva, W. Gu, G. Kim, R. Koster, R. Lucchesi, D. Merkova, J. Nielsen, G. Partyka, S. Pawson,
664 W. Putman, M. Rienecker, S. Schubert, M. Sienkiewicz, and B. Zhao, 2017: The Modern-Era
665 Retrospective Analysis for Research and Applications, Version 2 (MERRA-2). J. Climate.
666 doi:10.1175/JCLI-D-16-0758.1, in press.

667 Gordon, M., and Taylor, P. A.: Measurements of blowing snow, Part I: Particle shape, size
668 distribution, velocity, and number flux at Churchill, Manitoba, Canada, Cold Reg. Sci. Technol.,
669 55, 63-74, doi: 10.1016/j.coldregions.2008.05.001, 2009.

Harder, S. L., Warren, S. G., Charlson, R. J., and Covert, D. S.: Filtering of air through snow as a mechanism for aerosol deposition to the Antarctic ice sheet, J. Geophys. Res.-Atmos., 101, 18729-18743, doi: 10.1029/96jd01174, 1996.

Huang, N., Dai, X., and Zhang, J.: The impacts of moisture transport on drifting snow sublimation in the saltation layer, Atmos. Chem. Phys., 16, 7523-7529, doi:10.5194/acp-16-7523-2016, 2016.

Josset, D., Pelon, J., Garnier, A., Hu, Y. X., Vaughan, M., Zhai, P. W., Kuehn, R., and Lucker, P.: Cirrus optical depth and lidar ratio retrieval from combined CALIPSO-CloudSat observations using ocean surface echo, J. Geophys. Res.-Atmos., 117, doi: 10.1029/2011jd016959, 2012.

King, J. C., Anderson, P. S., and Mann, G. W.: The seasonal cycle of sublimation at Halley, Antarctica, J. Glaciol., 47, 1-8, doi: 10.3189/172756501781832548, 2001.

Lawson, R. P., Baker, B. A., Zmarzly, P., O'Connor, D., Mo, Q. X., Gayet, J. F., and Shcherbakov, V.: Microphysical and optical properties of atmospheric ice crystals at South Pole station, J. Appl. Meteor. Climatol., 45, 1505-1524, doi: 10.1175/Jam2421.1, 2006.

Lenaerts, J. T. M., van den Broeke, M. R., Dery, S. J., van Meijgaard, E., van de Berg, W. J., Palm, S. P., and Rodrigo, J. S.: Modeling drifting snow in Antarctica with a regional climate model: 1. Methods and model evaluation, J. Geophys. Res.-Atmos., 117, doi: 10.1029/2011jd016145, 2012a.

Lenaerts, J. T. M., van den Broeke, M. R., van de Berg, W. J., van Meijgaard, E., and Munneke, P. K.: A new, high-resolution surface mass balance map of Antarctica (1979-2010) based on regional atmospheric climate modeling, Geophys. Res. Lett., 39, doi: 10.1029/2011gl050713, 2012b.

Mahesh, A., Eager, R., Campbell, J. R., and Spinhirne, J. D.: Observations of blowing snow at the South Pole, J. Geophys. Res., 108(D22), 4707, doi:10.1029/2002JD003327, 2003.

694 Mann, G. W., Anderson, P. S., and Mobbs, S. D.: Profile measurements of blowing snow at
695 Halley, Antarctica, J. Geophys. Res.-Atmos., 105, 24491-24508, doi: 10.1029/2000jd900247,
696 2000.

697 Nishimura, K., and Nemoto, M.: Blowing snow at Mizuho station, Antarctica, Philos. T Roy Soc.
698 A, 363, 1647-1662, doi: 10.1098/rsta.2005.1599, 2005.

699 Palerme, C., Kay, J. E., Genthon, C., L'Ecuyer, T., Wood, N. B., and Claud, C.: How much snow
700 falls on the Antarctic ice sheet?, Cryosphere, 8, 1577-1587, doi: 10.5194/tc-8-1577-2014, 2014.

701 Palm, S. P., Yang, Y. K., Spinhirne, J. D., and Marshak, A.: Satellite remote sensing of blowing
702 snow properties over Antarctica, J. Geophys. Res.-Atmos., 116, doi: 10.1029/2011jd015828,
703 2011.

704 Pomeroy, J. W., Gray, D. M., and Landine, P. G.: The Prairie Blowing Snow Model -
705 Characteristics, Validation, Operation, J. Hydrol., 144, 165-192, doi: 10.1016/0022-
706 1694(93)90171-5, 1993.

707 Pomeroy, J. W., Marsh, P., and Gray, D. M.: Application of a distributed blowing snow model to
708 the arctic, Hydrol. Process, 11, 1451-1464, 1997.

709 Przybylak, R.: Recent air-temperature changes in the Arctic, Annals of Glaciology, Vol 46, 2007,
710 46, 316-324, doi: 10.3189/172756407782871666, 2007.

711 Rogers, R. R., and Yau, M. K.: A Short Course in Cloud Physics, 3rd. ed., Pergamon Press, 290 pp.,
712 1989.

713 Scarchilli, C., Frezzotti, M., Grigioni, P., De Silvestri, L., Agnoletto, L., and Dolci, S.: Extraordinary
714 blowing snow transport events in East Antarctica, Clim. Dynam., 34, 1195-1206, doi:
715 10.1007/s00382-009-0601-0, 2010.

716 Schmidt, R. A.: Vertical profiles of wind speed, snow concentration and humidity and blowing
717 snow, Boundary-layer Meteorol., 23, 223-246, 1982.

718 Steig, E. J., Schneider, D. P., Rutherford, S. D., Mann, M. E., Comiso, J. C., and Shindell, D. T.:
719 Warming of the Antarctic ice-sheet surface since the 1957 International Geophysical Year,
720 Nature, 457, 459-462, doi: 10.1038/nature07669, 2009.

721 Tabler, R. D., Benson, C. S., Santana, B. W., and Ganguly, P.: Estimating Snow Transport from
722 Wind-Speed Records - Estimates Versus Measurements at Prudhoe Bay, Alaska, Proceedings of
723 the Western Snow Conference : Fifty-Eighth Annual Meeting, 61-72, 1990.

724 Tabler, R. D.: Estimating the transport and evaporation of blowing snow Snow Management on
725 the Great Plains, July 1985, Swift Current, Sask, Great Plains Agricultural Council Publication No.
726 73, University of Nebraska, Lincoln, NE, 1975, pp. 85-105.

727 Trouvilliez, A., Naaim, F., Genthon, C., Piard, L., Favier, V., Bellot, H., Agosta, C., Palerme, C.,
728 Amory, C., and Gallée, H.: Blowing snow observation in Antarctica: A review including a new
729 observation system in Adélie Land, Cold Reg. Sci. Technol.,
730 doi:10.1016/j.coldregions.2014.09.005, 2014.

731 Van den Broeke, M., Konig-Langlo, G., Picard, G., Munneke, P. K., and Lenaerts, J.: Surface
732 energy balance, melt and sublimation at Neumayer Station, East Antarctica, Antarct. Sci., 22,
733 87-96, doi: 10.1017/S0954102009990538, 2010.

734 Walden, V. P., Warren, S. G., and Tuttle, E.: Atmospheric ice crystals over the Antarctic Plateau
735 in winter, J. Appl. Meteor. Climatol., 42, 1391-1405, doi: 10.1175/1520-
736 0450(2003)042<1391:Aicota>2.0.Co;2, 2003.

737 Winker, D. M., Vaughan, M. A., Omar, A., Hu, Y. X., Powell, K. A., Liu, Z. Y., Hunt, W. H., and
738 Young, S. A.: Overview of the CALIPSO mission and CALIOP data processing algorithms, J. Atmos.
739 Oceanic Technol., 26, 2310-2323, doi: 10.1175/2009jtecha1281.1, 2009.

740 Table I. The year average sublimation per year (average off all grid boxes) and the integrated
741 sublimation over the Antarctic continent (north of 82S). *2006 and 2016 consist of only 7 and 9
742 months of observations, respectively.

Year	Average Sublimation (mm swe)	Integrated Sublimation (Gt yr^{-1})
2006*	28.3 ±14.1	255 ± 128
2007	56.8 ± 28.4	514 ± 207
2008	49.2 ± 24.6	446 ± 223
2009	45.3 ± 22.6	409 ± 204
2010	42.9 ± 21.4	388 ± 194
2011	47.6 ± 23.8	431 ± 215
2012	44.4 ± 22.2	402 ± 201
2013	47.7 ± 23.8	432 ± 216
2014	41.5 ± 20.7	376 ± 188
2015	41.3 ± 20.6	374 ± 187
2016*	33.2 ± 16.6	301 ± 150
AVG	**43.5*** ± 21.7	**393.4*** ± 197

743

744 Table II. The total transport (Gt yr^{-1}) from continent to ocean for various regions in Antarctica
745 for 2007–2015.

746

747

748

749

Year	East Antarctica	West Antarctica	135E – 160E	80W – 120W
2007	2.52	1.29	1.72	0.82
2008	2.20	1.43	1.21	0.90
2009	2.63	1.27	1.51	0.78
2010	2.26	1.15	1.38	0.73
2011	2.04	1.04	1.13	0.64
2012	2.49	1.21	1.41	0.73
2013	2.54	1.41	1.26	0.83
2014	2.55	1.02	1.49	0.67
2015	2.76	1.38	1.58	0.69
Avg	**2.44**	**1.24**	**1.41**	**0.75**

750

751

752

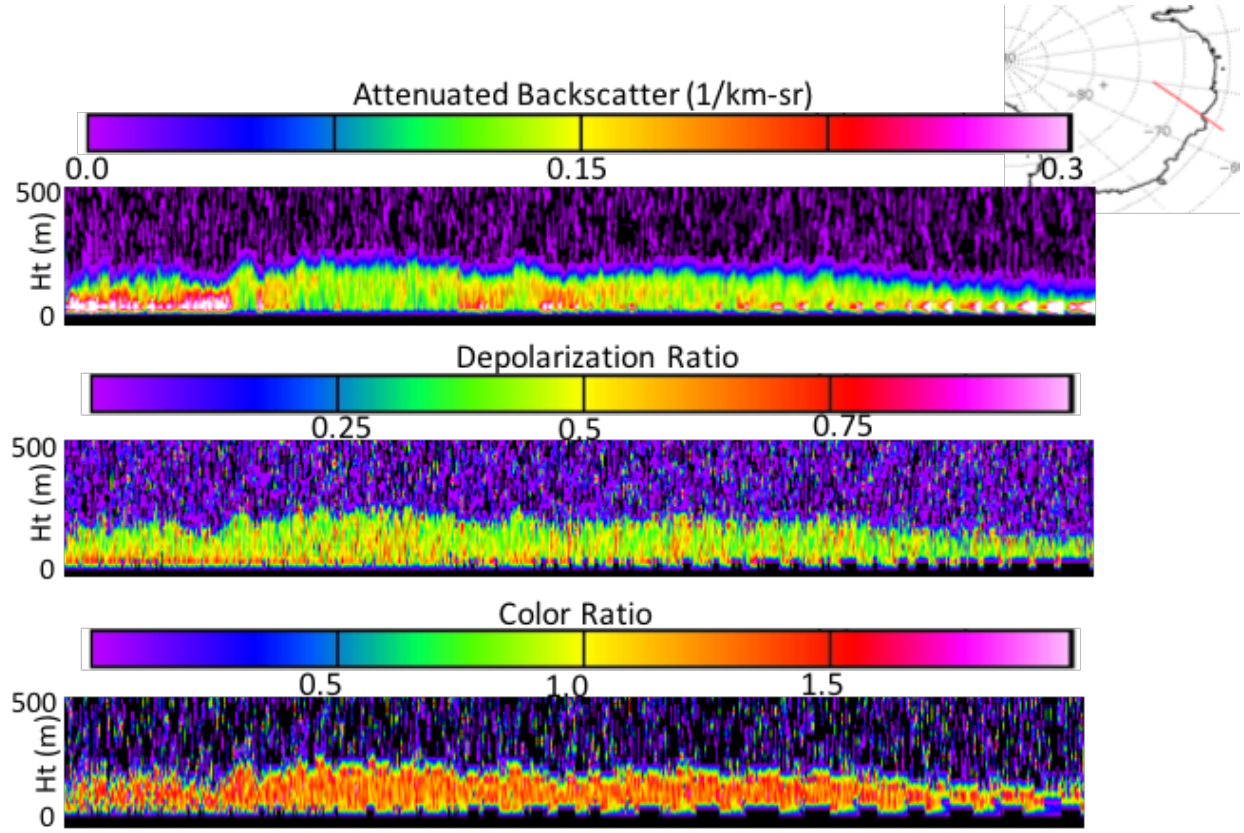

753

754 Figure 1. A typical Antarctic blowing snow layer as measured by CALIPSO on May 28, 2015 at
755 17:08:41 – 17:11:33 UTC. Displayed (from top to bottom) are the 532 nm calibrated, attenuated
756 backscatter, the depolarization ratio at 532 nm, and the color ratio (1064 nm / 532 nm).

757

758

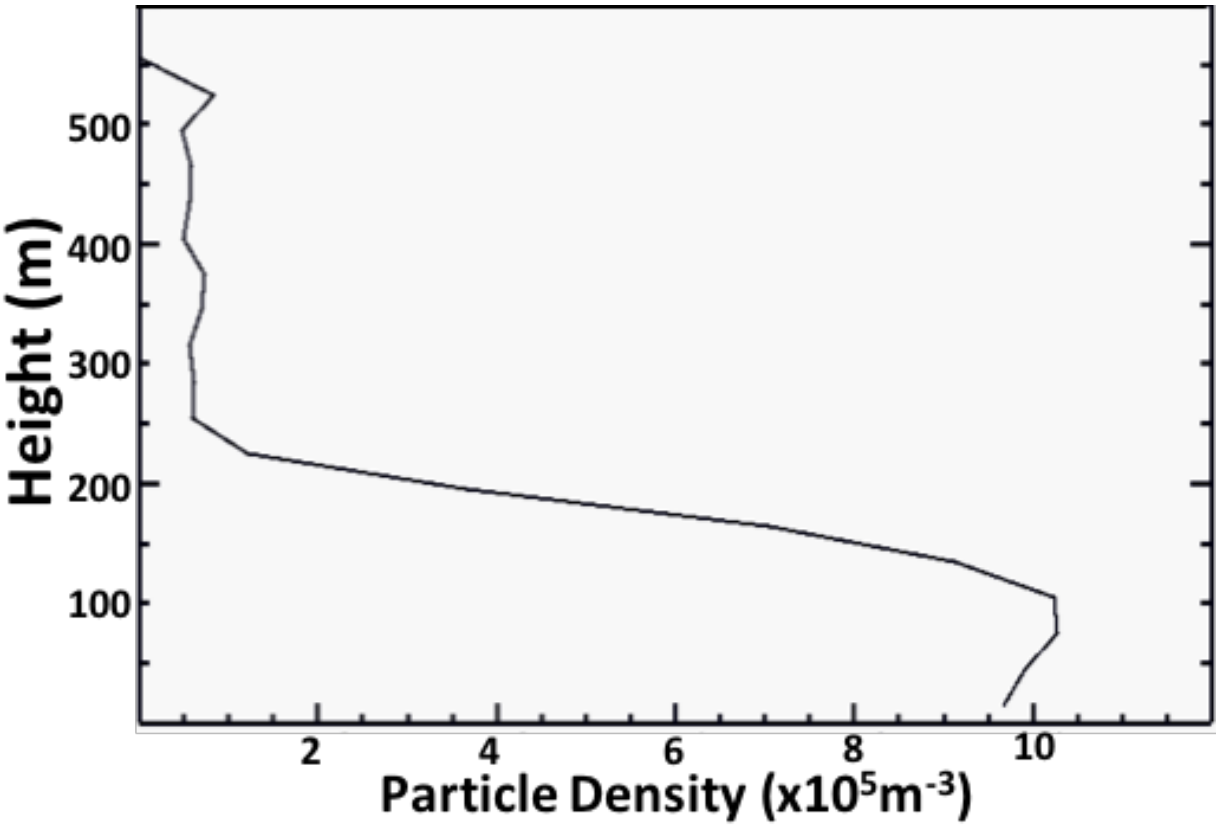

759

760 Figure 2. Average particle density profile (Eq. 2) through the blowing snow layer shown in Fig. 1.

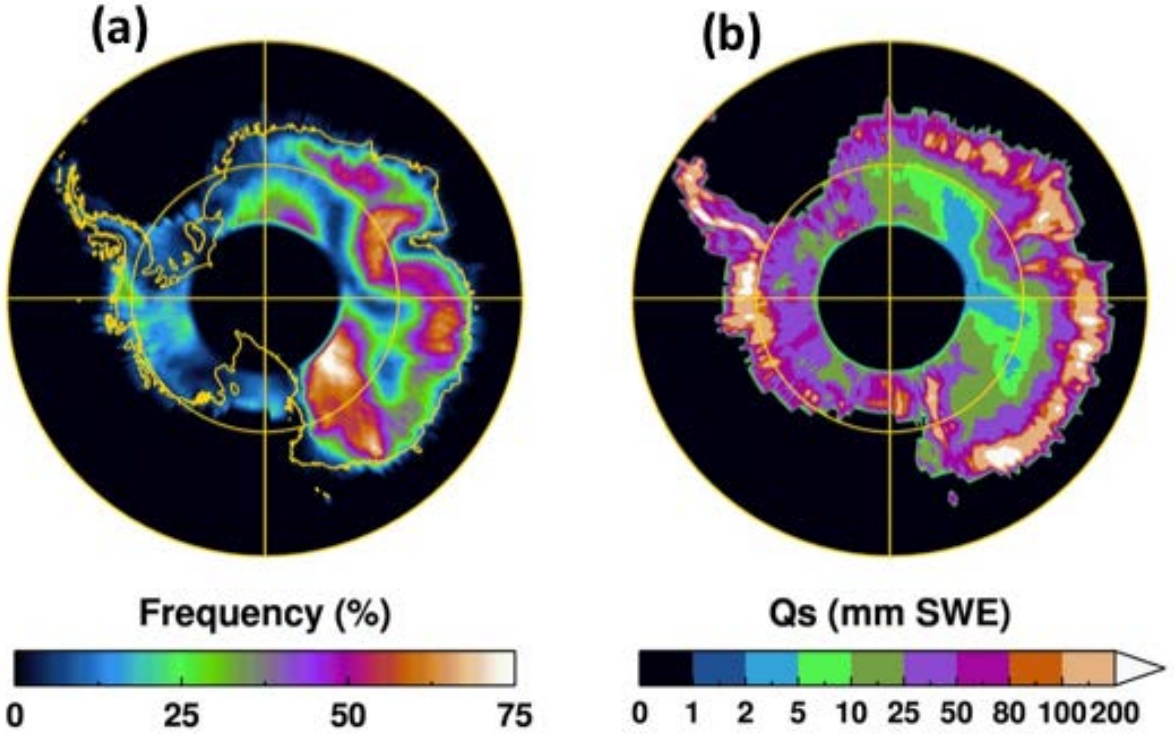

761

762 Figure 3. (a) The average April through October blowing snow frequency for the period 2007–
763 2015. (b) The average annual blowing snow sublimation for the same period as in (a).

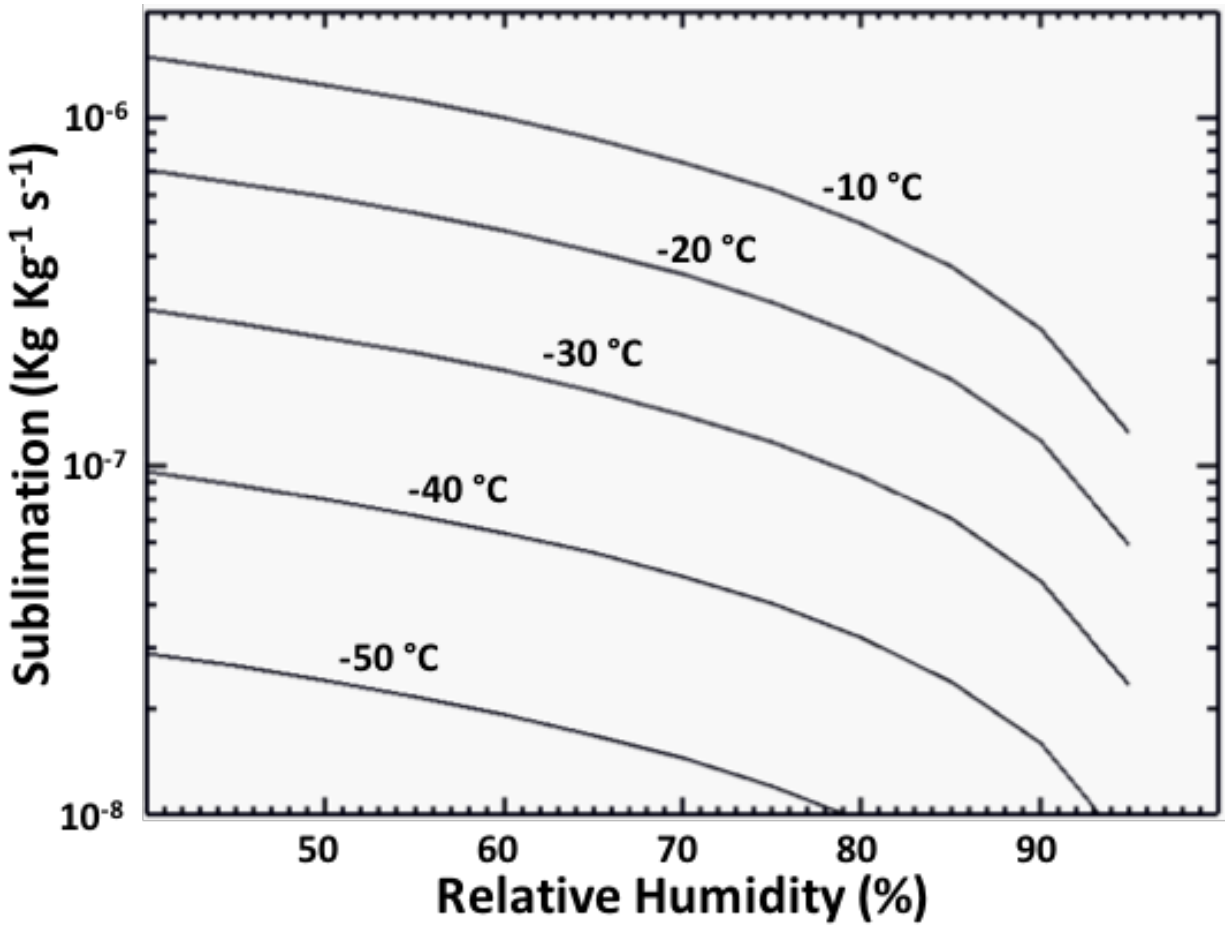

764

765 Figure 4. Computed blowing snow sublimation rate using Eqs. (3) and (4) as function of relative
766 humidity for varying air temperatures. The particle density value used in Eq. (3) was 10^6 m^{-3}
767 which corresponds to a blowing snow mixing ratio (qb) of 4.7x10-5 kg kg^{-1}

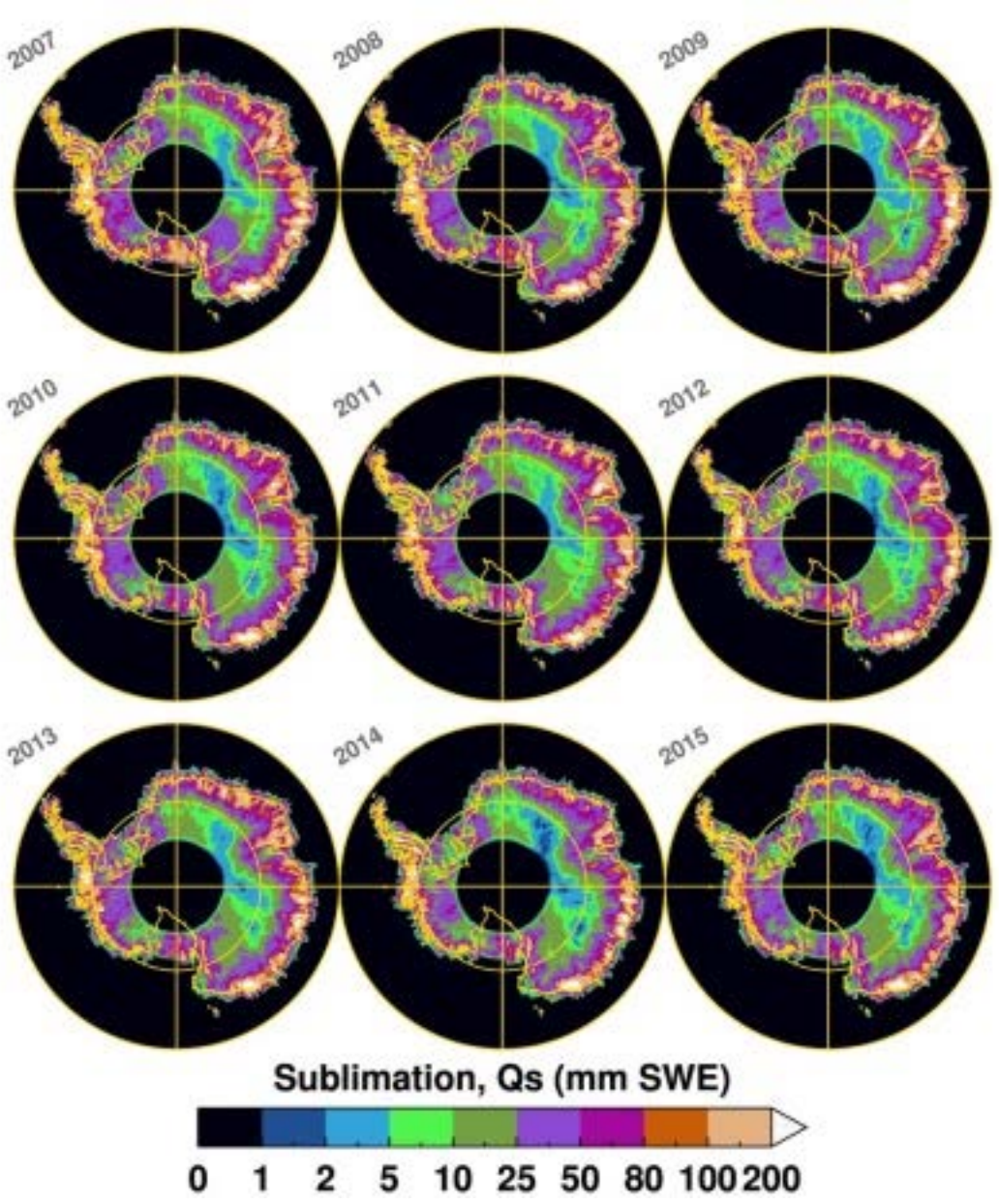

768

769 Figure 5. Blowing snow total sublimation over Antarctica by year for 2007–2015.

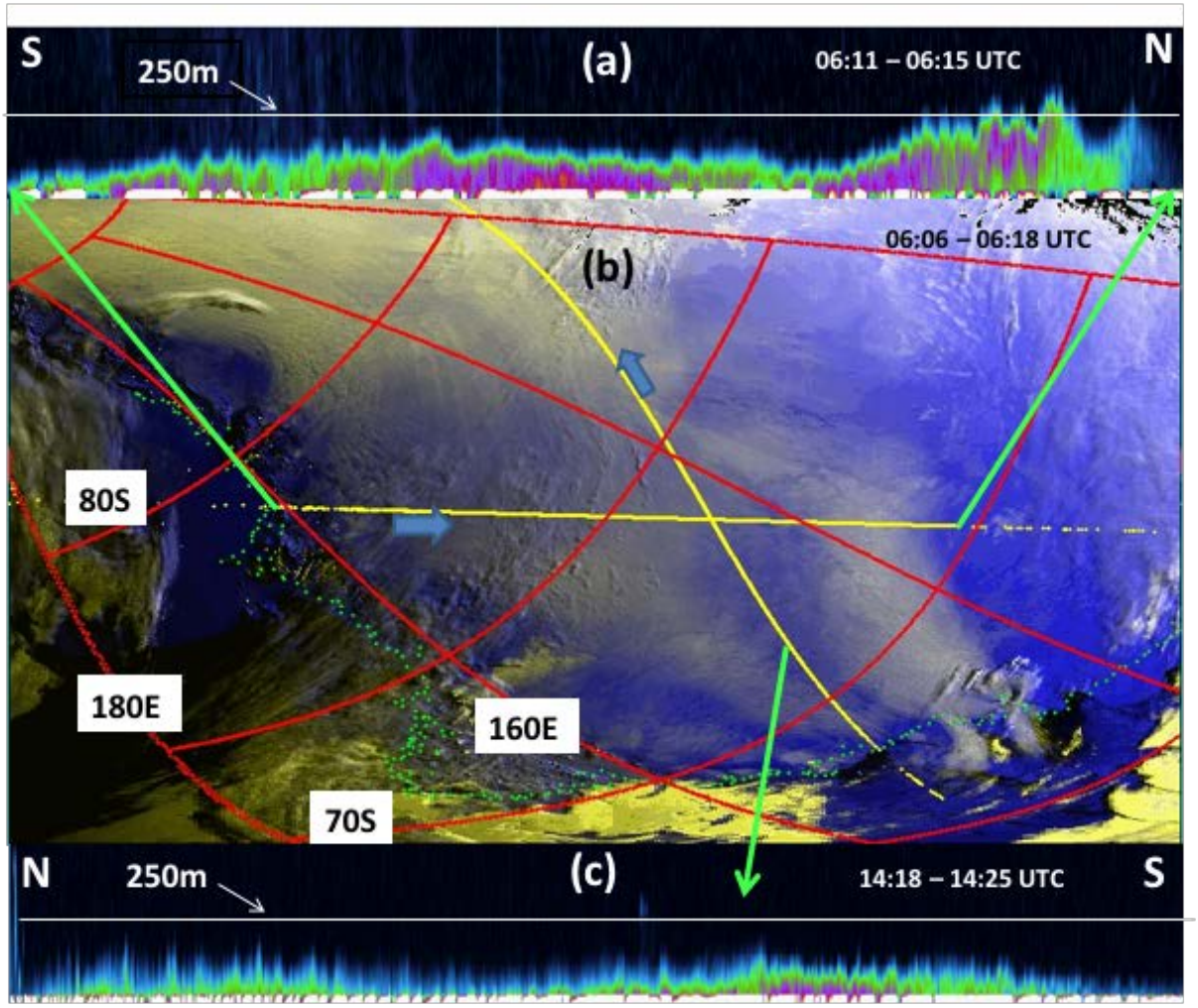

770

771 Figure 6. A large blowing snow storm over Antarctica with blowing snow transport from
772 continent to ocean on October 14, 2009. (a) CALIOP 532 nm attenuated backscatter along the
773 yellow (south to north) line bounded by the green arrows as shown in (b) at 06:11 – 06:15 UTC.
774 (b) MODIS false color image at 06:06:14 – 06:17:31 UTC showing blowing snow as dirty white
775 areas. The coastline is indicated by the green dots, and two CALIPSO tracks, where blowing
776 snow was detected are indicated by the yellow lines. (c) CALIOP 532 nm attenuated backscatter
777 along the yellow (north to south) line, 14:18 – 14:25 UTC.

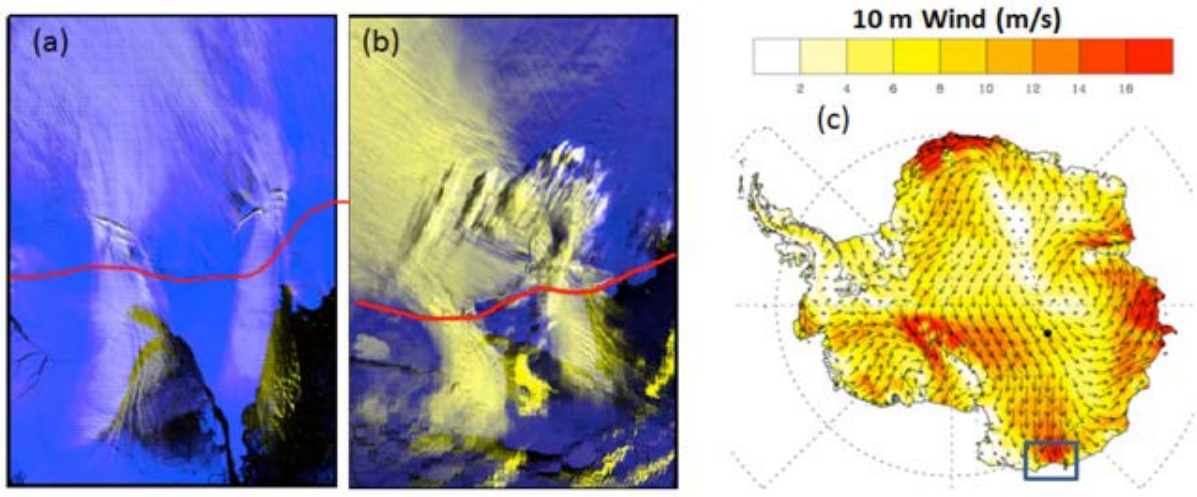

778

779 Figure 7. (a) MODIS false color image on October 13, 2009, 23:00 UTC and (b) October 14, 2009,
780 06:16 UTC. The red line is the approximate position of the coastline. (c) The 10 m wind speed
781 from the AMPS model (Antarctic Mesoscale Prediction System) for October 14, 2009. The area
782 covered by the MODIS images is roughly that indicated by the blue box in (c).

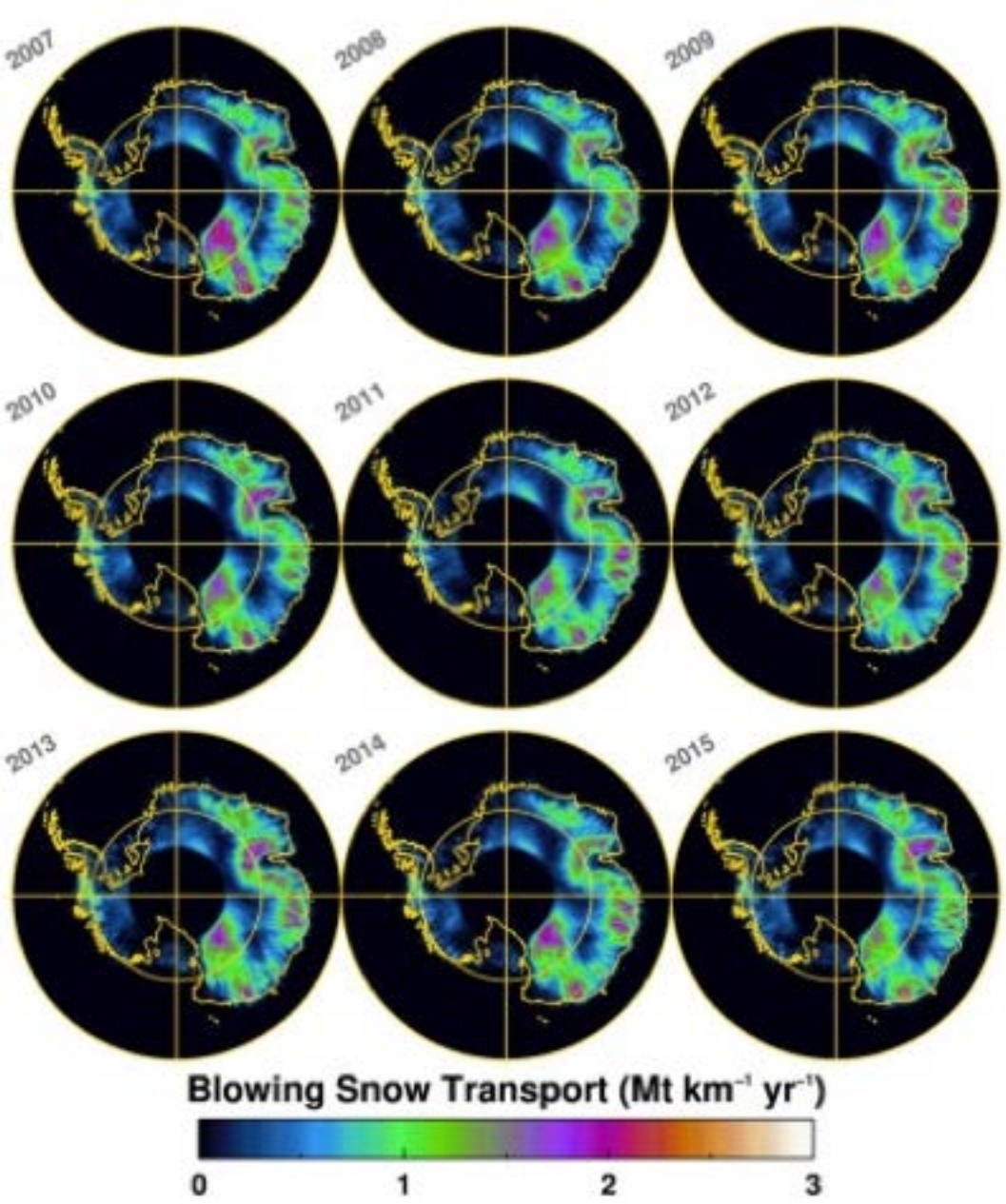

783

784 Figure 8. The magnitude of blowing snow transport over Antarctica integrated over the year for
785 years 2007–2015.

786

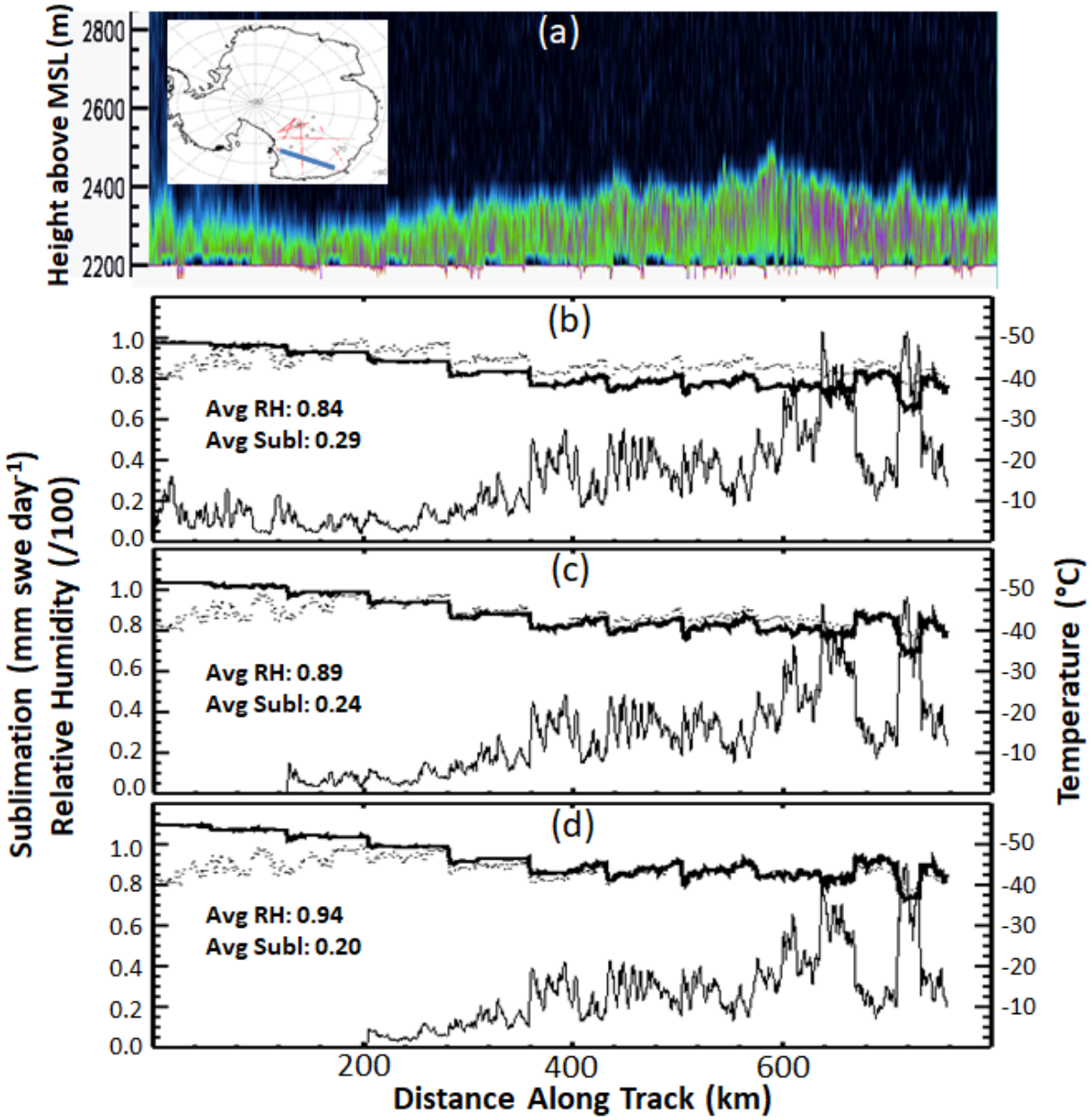

787

788 Figure 9. (a) CALIPSO backscatter showing blowing snow layer along the blue line in the map
789 inset on 10/12/2010 at 05:51 UTC. (b) Average MERRA-2 moisture (dark black line),
790 temperature (dotted line) and calculated sublimation through the blowing snow layer along the
791 CALIPSO track. (c and d) Same as in (b) but increasing MERRA-2 humidity by 5 and 10%,
792 respectively.

793